



Cite this: DOI: 10.1039/c9md00096h

Discovery of 2-phenoxyacetamides as inhibitors of the Wnt-depalmitoleating enzyme NOTUM from an X-ray fragment screen†‡§

Benjamin N. Atkinson,[¶] David Steadman,[¶] Yuguang Zhao,[¶] James Siphthorp,[¶] Luca Vecchia,[¶] Reinis R. Ruza,[¶] Fiona Jeganathan,^a Georgie Lines,^a Sarah Frew,^a Amy Monaghan,^a Svend Kjær,^c Magda Bictash,^a E. Yvonne Jones^{¶*} and Paul V. Fish^{¶*ac}

NOTUM is a carboxylesterase that has been shown to act by mediating the *O*-depalmitoleoylation of Wnt proteins resulting in suppression of Wnt signaling. Here, we describe the development of NOTUM inhibitors that restore Wnt signaling for use in *in vitro* disease models where NOTUM over activity is an underlying cause. A crystallographic fragment screen with NOTUM identified 2-phenoxyacetamide **3** as binding in the palmitoleate pocket with modest inhibition activity (IC₅₀ 33 μM). Optimization of hit **3** by SAR studies guided by SBDD identified indazole **38** (IC₅₀ 0.032 μM) and isoquinoline **45** (IC₅₀ 0.085 μM) as potent inhibitors of NOTUM. The binding of **45** to NOTUM was rationalized through an X-ray co-crystal structure determination which showed a flipped binding orientation compared to **3**. However, it was not possible to combine NOTUM inhibition activity with metabolic stability as the majority of the compounds tested were rapidly metabolized in an NADPH-independent manner.

Received 15th February 2019,
Accepted 11th April 2019

DOI: 10.1039/c9md00096h

rsc.li/medchemcomm

Members of the Wnt family are secreted signaling proteins that play key roles in adult stem cell biology as well as in embryonic development.¹ Wnts initiate signaling by binding to cell surface receptors and two main pathways have been identified downstream of Wnts: the so-called ‘canonical’ and ‘planar cell polarity’ pathways. These pathways are triggered

by the binding of Wnt to a member of the Frizzled family of cell surface receptors and, for the canonical pathway, a member of the LDL-receptor-related protein (LRP) family of cell surface receptors (typically LRP5 or LRP6). This binding elicits an intracellular signaling cascade that results in both biochemical and transcriptional changes within the cell, with the canonical pathway involving the accumulation and translocation of β-catenin. Both pathways are tightly regulated by a sophisticated network of modulators and feedbacks including secreted inhibitory Dickkopf (DKK) proteins² and post translational modifications (PTM).^{3,4}

Conversely, dysregulation of Wnt signaling is frequently associated with growth-related pathologies and cancers,⁵ particularly those of tissues for which Wnts normally stimulate self-renewal and repair. Wnt signaling is also implicated to have a role in neurodegenerative diseases such as Alzheimer’s disease (AD). Cognitive impairments, characteristic of AD, correlate closely with the loss of synapses and current knowledge suggests that excess amyloid-β (Aβ) causes synapse dysfunction by impairing synapse maintenance, at least in part, through causing dysfunction of Wnt signaling.^{6,7} Compromised Wnt signaling may also be associated with AD through loss of blood–brain barrier (BBB) integrity⁸ and Aβ generation through β-secretase (BACE1) expression.⁹

O-Palmitoleoylation of a conserved serine residue in Wnt proteins is a key PTM required for efficient binding of Wnt proteins to Frizzled receptors, a requirement for signal

^a Alzheimer’s Research UK UCL Drug Discovery Institute, University College London, Cruciform Building, Gower Street, London, WC1E 6BT, UK.

E-mail: p.fish@ucl.ac.uk; Tel: +44 (0)20 7679 6971

^b Division of Structural Biology, Wellcome Centre for Human Genetics, University of Oxford, The Henry Wellcome Building for Genomic Medicine, Roosevelt Drive, Oxford, OX3 7BN, UK. E-mail: yvonne@strubi.ox.ac.uk; Tel: +44 (0)1865 287 546

^c The Francis Crick Institute, 1 Midland Road, London, NW1 1AT, UK

† This work was first presented at the following international conferences: E. Y. J. Biochemical Society Meeting. Acylation of intracellular and secreted proteins: mechanisms and functional outcomes; 10–12th September 2018; Brighton, UK. P. V. F. EFMC: XXVth International Symposium on Medicinal Chemistry; 2–6th September 2018; Ljubljana, Slovenia.

‡ Electronic supplementary information (ESI) available: Synthetic procedures and characterization data; enzyme production and purification methods; OPTS assay procedure; FP-biotin competition assay; TCF/LEF reporter assay; ADME screens; protein crystallization, data collection and structure determination. See DOI: 10.1039/c9md00096h

§ Atomic coordinates have been deposited in the Protein Data Bank (PDB) and will be released upon publication. PDB ID codes: **3**: 6R8P; **39**: 6R8Q; **45**: 6R8R.

¶ B. N. A., D. S. and Y. Z. contributed equally. The manuscript was written through contributions from all authors. B. N. A., D. S., J. S., A. M., E. Y. J. and P. V. F. wrote the manuscript. All authors have given approval to the final version of the manuscript.



transduction.¹⁰ A carboxylesterase NOTUM was previously shown to antagonize Wnt signaling pathways.¹¹ More recently, NOTUM has been shown to act by mediating the depalmitoleoylation of Wnt proteins resulting in suppression of Wnt signaling.^{12,13} It follows that inhibition of NOTUM could restore Wnt signaling with potential benefit in disease where Wnt deficiency is an underlying cause.

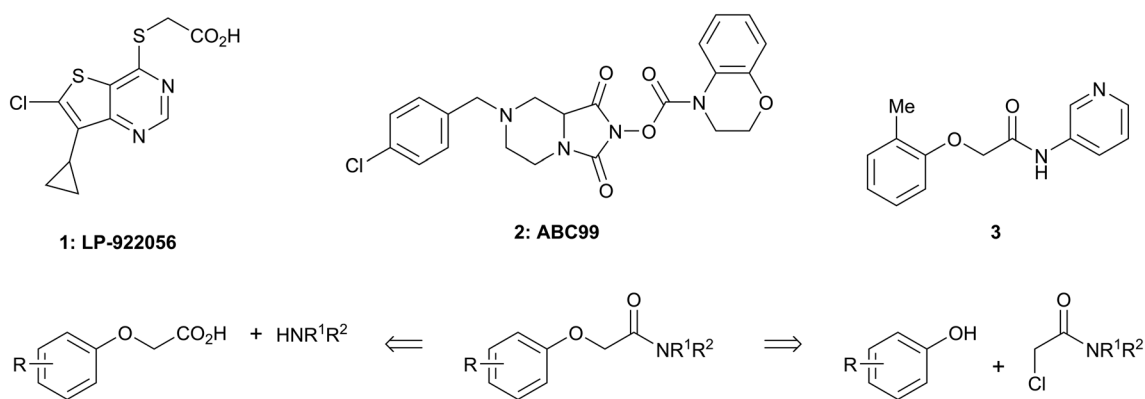
There are only a few reports of NOTUM inhibitors with compounds falling into two main categories (Scheme 1). Thienopyrimidine LP-922056 (**1**) is a potent, orally active inhibitor of NOTUM that has shown NOTUM to be a potential drug target for stimulating bone formation and treating osteoporosis.¹⁴ However, although **1** demonstrates low clearance and good bioavailability, the structure contains an essential carboxylic acid and acids tend to have low passive brain penetration;^{15–18} in fact, it is an accepted strategy to add a carboxylic acid group to minimize brain penetration of drugs for peripheral targets.¹⁹ *N*-Hydroxyhydantoin carbamates are potent and selective irreversible inhibitors of NOTUM discovered by activity-based protein profiling (ABPP).²⁰ An optimized inhibitor ABC99 (**2**) preserves Wnt-mediated cell signaling in the presence of NOTUM and was converted to a clickable ABPP probe for visualizing NOTUM in biological systems. Due to their reactive mechanism of action forming covalent adducts with NOTUM Ser232, it is unlikely that these compounds will be suitable for *in vivo* studies. Hence, our objective was to discover potent small molecule inhibitors of NOTUM suitable for exploring the regulation of Wnt signaling in the central nervous system (CNS) and modulation of AD phenotypes.

In order to identify new small molecule inhibitors of NOTUM, a crystallographic fragment screen was performed using the XChem platform at Diamond Light Source. Crystals of C-terminal his-tagged NOTUM(Ser81-Thr451 Cys330Ser) were soaked with the DSI-Poised library (XChem, 768 fragments).²¹ Crystal structures of NOTUM show a distinctive pocket that accommodates the palmitoleate group (Fig. 1A).¹² Fragments observed to bind in the palmitoleate pocket were all re-synthesized as solid samples to establish structure and purity. Inhibition of NOTUM carboxylesterase activity of these

hits was measured in a cell-free biochemical assay. In brief, test compounds (dispensed to give 10 point concentration–response-curves) were incubated with NOTUM(81-451 Cys330Ser) and trisodium 8-octanoyloxyppyrene-1,3,6-trisulfonate (OPTS) as the substrate for 1 h, and fluorescence recorded; an inhibitor of NOTUM would suppress fluorescence by binding to NOTUM and preventing hydrolysis of OPTS (ESI,† Fig. S1).^{14,22}

One of the preferred hits from this set was 2-(2-methylphenoxy)-*N*-(pyridine-3-yl)acetamide (**3**) (IC₅₀ 33 ± 4.7 μM) which was selected for further investigation for several reasons: (1) excellent “hit-like” properties (mw 242; clog *P* 1.7; TPSA 51; LE = 0.35; LLE = 2.8) with no obvious reactive groups; (2) chemically enabled to selectively functionalize each position to explore structure activity relationships (SAR); (3) successful co-crystal structure with NOTUM to support a structure based drug design (SBDD) program; and (4) structural features and physicochemical properties consistent with CNS drug-like space²³ including a favorable ‘CNS multiparameter optimization’ (CNS MPO) score (CNS MPO = 5.6/6.0).^{24,25} Analysis of the crystal structure (Fig. 1B) showed key pi–pi stacking interactions between the pyridine ring and Trp128 at the outer pocket, and further pi–pi interactions between the tolyl ring and Phe268/Phe320 within the deeper, lipophilic pocket. No hydrogen bonding interactions between the ligand and the protein were observed, so it was considered that these pi–pi interactions were crucial for binding, in addition to general lipophilic interactions, as observed for the palmitoleate ligand (Fig. 1A). Notably, the orientation of Trp128 is significantly shifted in our crystal structures compared to previous structures like PDB 4UZQ. This shift shows a more open form of the binding site. Also in contrast to the *O*-palmitoleoyl serine structure, **3** does not interact with the oxyanion hole of the active site.

Two general synthetic methods were used to prepare new analogues: either an activated amide coupling reaction between the aminoheterocycle and the 2-phenoxyacetic acid; or a nucleophilic substitution reaction between the 2-chloroacetamide and the relevant phenoxide (Scheme 1; see, ESI†). Inhibition of NOTUM carboxylesterase activity was



Scheme 1 Chemical structures of LP-922056 (**1**), ABC99 (**2**) and initial fragment hit **3**. General scheme for the synthesis of 2-phenoxyacetamides reported in Tables 1 and 2.



routinely measured in an OPTS biochemical assay as described above. Selected compounds were then screened for NOTUM occupancy in a FP-biotin competition assay²⁶ and/or inhibition of NOTUM activity in a Wnt/ β -catenin signaling pathway TCF/LEF reporter (luciferase) HEK293 cell line with exogenous Wnt3a and NOTUM.^{14,22} Compounds were also screened for aqueous solubility, transit performance in MDCK-mdr1 cell lines for permeability, and metabolic stability in human and mouse liver microsomes (HLM and MLM resp.) as a measure of clearance.

The SARs were directed at exploring four principle areas of the original hit 3: the 2-heteroatom linker (4–7), substituents on the phenoxy ring (8–18), the acetamide backbone (19, 20) (Table 1), and the amide group (21–53) (Table 2). Furthermore, target compounds were designed to have molecular and physicochemical properties consistent with CNS drug-like space. It is generally accepted that CNS drugs tend to occupy a restricted property space compared to general orally available drugs,²³ and extensive efforts have been made to define attributes that are desirable for molecules to have good brain exposure. One such model is the CNS MPO score^{24,25} which we routinely used in our compound design. A second useful design metric was lipophilic ligand efficiency (LLE)^{27,28} used to track improvements in NOTUM activity against lipophilicity ($\log P$) of the inhibitors. The palmitoleate pocket of NOTUM is a very lipophilic environment and we were keen to avoid gains in activity simply through increased compound lipophilicity.

Initial studies suggested that replacing the O-atom linker was not an effective strategy for increasing activity, with po-

tency decreasing from O > NH > S > CH₂ (3–6) (Table 1). The preference for an O-linker was believed to be due to a favorable internal H-bond with the amide NH holding the molecule in a low energy conformation that closely mimicked the NOTUM binding conformation. The NMe linker 7 was similar in potency for this matched pair (3 vs. 7) although this did not prove to be a general trend, and so the O-linker was retained for the next phase of SAR. *N*-Methylation of the amide group (19) or the 2-phenoxy propanamide backbone (20) was tolerated but offered no advantage (Table 1).

Guided by the NOTUM-3 crystal structure, a concise investigation of SAR of the phenoxy ring indicated the original 2-methyl group in 3 was preferred with a beneficial 2-fold increase in potency only achieved by direct replacement with a 2-chlorine atom 13 (Table 1). Moving the Cl atom or Me group to the 3-, 4-positions gave a significant decrease in potency (14, 15, 16) and was not pursued further at this point. These results were consistent with the structural information showing minimal space to accommodate any group larger than H- or F-atom (17) in these positions. The symmetrical 2,6-diMe phenoxy ether 18 was tolerated but offered no advantage over a single 2-Me substituent. From this limited set, most groups were detrimental, or offered little advantage, compared to having no substituent (8; R = H) with a preference for small lipophilic groups at the 2-position of the ring such as 2-Me, 2-Cl and 2-CF₃.

The next phase of SAR was to explore the *N*-acetamide substituent with a variety of heterocycles (Table 2). Although swapping the 3-Py group for the Ph (21) gave a boost in activity, this was at a significant penalty in added lipophilicity

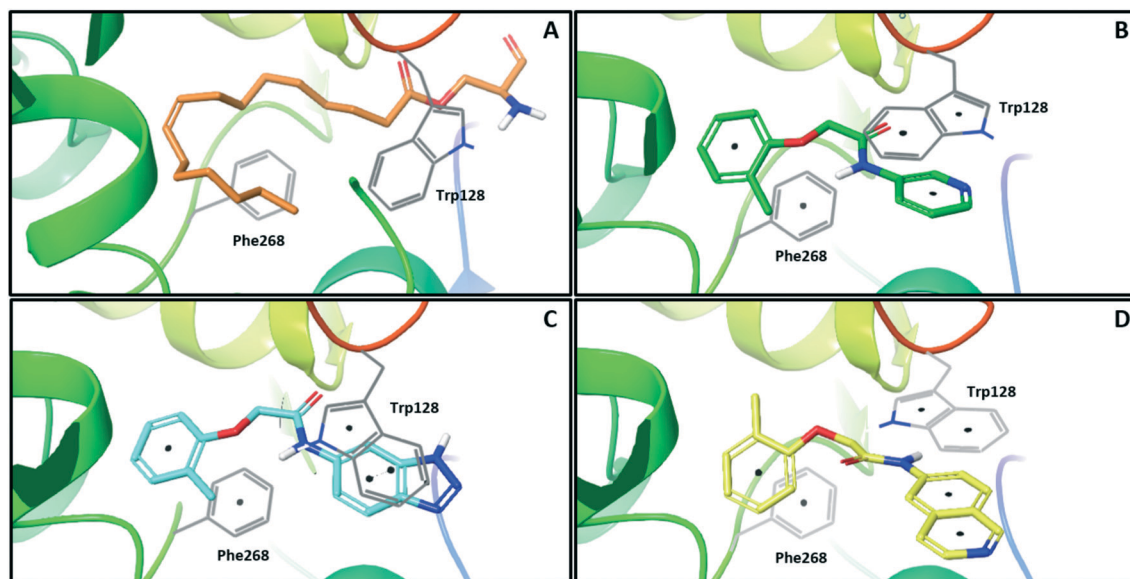


Fig. 1 X-ray crystal structures of ligands bound to NOTUM. (A) *O*-Palmitoleoyl serine (orange) (S232A mutant NOTUM), PDB ID: 4UZQ; (B) fragment hit 3 (green) with key π - π stacking interactions between the ligand and Trp128 and Phe268 indicated, PDB ID: 6R8P; (C) benzotriazole 39 (blue) showing a similar binding mode to 3, but with flipping of Trp128, PDB ID: 6R8Q; (D) isoquinoline 45 (yellow) demonstrates a reorientation of the phenoxy and amide groups but with key π - π stacking interactions maintained, PDB ID: 6R8R. Ligands are shown as sticks, and protein represented as ribbons with key amino acids shown as lines. Key π - π stacking interactions are shown between the ligands and the protein as black dots. Phe320 lies above the plane of the figure and is not shown for clarity.



Table 1 Inhibition of NOTUM activity. SAR of the heteroatom linker, the phenoxy ring and the acetamide


#	X	R	IC ₅₀ ^a (μM)
3	O	2-Me	33
4	NH	2-Me	60
5	S	2-Me	110
6	CH ₂	2-Me	140
7	NMe	2-Me	23
8	O	H	150
9	O	2-F	290
10	O	2-OMe	170
11	O	2-CN	120
12	O	2-CF ₃	37
13	O	2-Cl	14
14	O	3-Cl	310
15	O	3-Me	37% I @ 100 μM
16	O	4-Me	20% I @ 100 μM
17	O	2-Me;4-F	20
18	O	2-Me;6-Me	44
19	—	—	180
20	—	—	100

^a Values are geometric means of $n = 2-8$ experiments quoted to 2 s.f. Screening data only passed the quality control criteria if the screening plates demonstrated a $Z' > 0.5$ and the NOTUM inhibition activity of the positive control was within acceptable limits (IC₅₀ 0.6–1.1 nM). Differences of <2-fold should not be considered significant. See also ESI Table S1 for s.e.m.

(*clogP* 2.9, LLE = 2.8), and pyrazine 22 proved to be a more efficient inhibitor (*clogP* 0.8, LLE = 4.2). Interestingly, the 3-(aminomethyl)pyridine amide 25 showed a decrease in potency from 3 suggesting that the introduction of the methylene linker disrupted the positioning of the ligand. The most significant increase in activity was achieved with benzo-fused heterocycles such as 26 and 27. These results prompted a more systematic investigation of both 6,5- and 6,6-heterocycles.

Fused 6,5-ring systems were well tolerated, with a range of indoles (28, 29), benzimidazoles (30, 31), indazoles (32–38) and benzotriazoles (39–41) having NOTUM inhibition <1 μM (Table 2). With good activity now achieved within this series, indazole 34 (IC₅₀ 0.27 ± 0.06 μM) (*clogP* 3.1; LLE 3.6; CNS MPO 5.6) was selected as a representative early lead for *in vitro* ADME profiling. Indazole 34 had low aqueous thermodynamic solubility (2 μg mL⁻¹) and moderate cell permeability as measured by transit performance in the MDCK-mdr1 cell line with no evidence of P-gp mediated efflux (AB/BA P_{app} 5.1/6.6 × 10⁶ cm s⁻¹). However, 34 had very poor metabolic stability in both HLM and MLM and was found to be rapidly degraded in a NADPH-independent manner (Table 3). Hydrolytic stability of 34 was tested in three buffer systems (pH 4, 7.4, 10) at multiple time points up to 18 h and only

parent was detected by UPLC-MS confirming degradation of 34 was not caused by simple hydrolysis. These results highlighted the need to further improve NOTUM inhibition activity whilst simultaneously developing compounds with good metabolic stability. Hence the microsomal stability assay became a priority secondary screen (*vide infra*).

Further investigation of SAR within the indazole series showed activity was increased by addition of a larger alkyl group (Me, Et, *iPr*) on the N1 or N2 position (35 vs. 37 vs. 38). Particularly noteworthy is the 2-isopropylindazole 38 (IC₅₀ 0.032 ± 0.004 μM) (*clogP* 4.0; LLE 3.5; CNS MPO 5.1) which was the most potent NOTUM inhibitor from this 6,5-series. Benzotriazoles (39–41) were well tolerated with the SAR of the N1-Me (40) and N2-Me (41) derivatives tracking their counterparts in the indazole series (*e.g.* 32 vs. 35 vs. 41). The unsubstituted benzotriazole 39 (IC₅₀ 0.12 ± 0.04 μM) (*clogP* 2.8; LLE 4.2; CNS MPO 5.0) offered a slight advantage and again showed that a free N1-H could be accommodated as seen previously with indole 26. However, both 38 and 39 were also rapidly degraded in HLM and MLM in a NADPH-independent manner.

Fused 6,6-ring systems showed more variation in their NOTUM inhibition activities with the position of the N atom(s) critical for achieving good activity (Table 2). A systematic migration of a single N atom around each available position of the heterocycle (42–48) showed a preference for the N atom in the distal ring with a clear advantage for the 6-isoquinoline isomer 45 (IC₅₀ 0.085 ± 0.011 μM) (*clogP* 3.0; LLE 4.1; CNS MPO 5.6). Multiple N atoms were accommodated in the distal ring of the 6,6-rings as shown with quinazoline 49 but was still inferior to 45.

With good NOTUM inhibition activity achieved across a range of amides, preferred compounds (IC₅₀ < 0.50 μM) were submitted for NOTUM X-ray co-crystallography studies to elucidate their binding modes. Structures of benzotriazole 39 (Fig. 1C) and isoquinoline 45 (Fig. 1D) were solved and showed that, while having similar potencies, they differed in their adopted binding conformations. Both compounds formed π-π stacking interactions with Trp128 through their heterocyclic rings but there was a distinct difference in the orientation of their phenoxyacetamide backbones. Benzotriazole 39 adopted a similar orientation as the pyridinyl fragment 3 (Fig. 1B). In contrast, isoquinoline 45 showed a 180° rotation around the amide bond with the carbonyl oxygen now pointing away from the oxyanion hole and the methyl group of the tolyl group occupying the opposite side of the lipophilic pocket.

An overlay of the crystal structures of 3 and 45 showed that the phenoxy ring of 45 was shifted slightly (*ca.* 1.28 Å) towards the front of the binding pocket, suggesting the possibility of additional space for further modification to this ring. Therefore, substitution on the phenoxy ring was revisited in the 45 series in an attempt to achieve optimal occupancy of the lipophilic pocket and increase potency. However, once again, only a 2-Cl group 50 (IC₅₀ 0.069 ± 0.011 μM) (*clogP* 3.3; LLE 3.9; CNS MPO 5.5) was accommodated with the 3-Me 51 and 3-Cl 52 giving a significant decrease in potency,

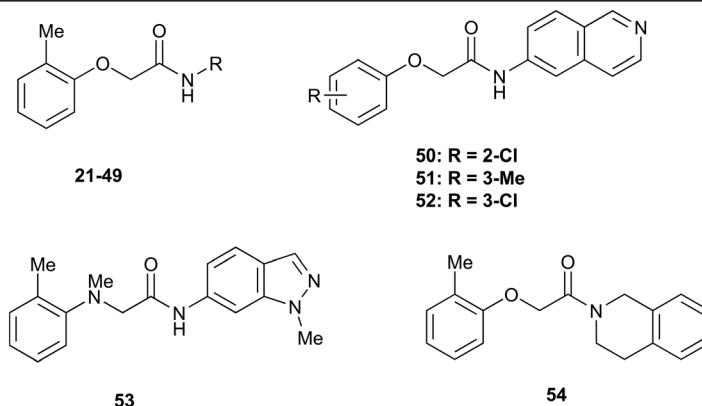


Table 2 Inhibition of NOTUM activity. SAR of the amide heterocycles

#	R	IC ₅₀ ^a (μM)	#	R	IC ₅₀ ^a (μM)
21-49			50: R = 2-Cl		
			51: R = 3-Me		
			52: R = 3-Cl		
53			54		
3		33	21		1.6
22		9.4	23		3.6
24		72	25		100
26		0.21	27		0.68
28		0.33	29		0.24
30		0.52	31		0.98
32		0.36	33		0.27
34		0.27	35		0.28
36		0.20	37		0.068
38		0.032	39		0.12
40		0.44	41		0.27
42		7.4	43		2.5



Table 2 (continued)



#	R	IC ₅₀ ^a (μM)	#	R	IC ₅₀ ^a (μM)
44		1.2	45		0.085
46		0.97	47		0.43
48		15	49		0.67
50	—	0.069	51	—	19
52	—	5.2	53	—	5.7
54	—	7.9			

^a Values are geometric means of $n = 2-8$ experiments quoted to 2 s.f. Screening data only passed the quality control criteria if the screening plates demonstrated a $Z' > 0.5$ and the NOTUM inhibition activity of the positive control was within acceptable limits (IC₅₀ 0.6–1.1 nM). Differences of <2-fold should not be considered significant. See also ESI Table S1 for s.e.m.

Table 3 *In vitro* microsomal stability data for selected compounds

#	NOTUM IC ₅₀ (μM)	HLM ($t_{1/2}$ min)	MLM ($t_{1/2}$ min)	clogP
3	33	—	1.1 ^a	1.7
22	9.4	—	Not detected ^a	0.8
34	0.27	11.6 ^a	Not detected ^a	3.1
38	0.032	5.1 ^a	5.7 ^a	4.0
39	0.12	—	1.8 ^a	2.8
45	0.085	12.1 ^a	11.0 ^a	3.0
50	0.069	—	3.3 ^a	3.3
53	5.7	—	5.2 ^a	3.1
54	7.9	—	Not detected ^a	3.5

^a NADPH independent metabolism.

although still superior to the direct analogues in the 3-pyridinyl series (14 and 15). Isoquinoline amides 45 and 50 were screened in liver microsomes and also showed rapid degradation in a NADPH-independent manner.

Representative inhibitors were tested in a NOTUM occupancy assay using FP-biotin, a serine hydrolase activity-based probe, whereby labelling of NOTUM with FP-biotin can be blocked by an inhibitor occupying the active site of NOTUM (Fig. 2A). All inhibitors showed some ability to prevent labelling by FP-biotin, confirming they competitively bind to NOTUM, albeit with modest potency compared to 1, and the

rank order of binding tracks with NOTUM IC₅₀ activity in the OPTS assay.

Preferred inhibitors were then screened in the cell-based TCF/LEF reporter gene (Luciferase) assay to assess their ability to restore Wnt/β-catenin signaling when activated by exogenous Wnt3a (100 ng mL⁻¹) in the presence of NOTUM (500 ng mL⁻¹) (Fig. 2B). Assay validation studies with a training set of NOTUM inhibitors showed that nanomolar activity in the OPTS assay (IC₅₀ < 1 μM) was required to show activity in the cell assay; these findings are consistent with previous reports.^{14,22} Compound 1 showed an effective activation of



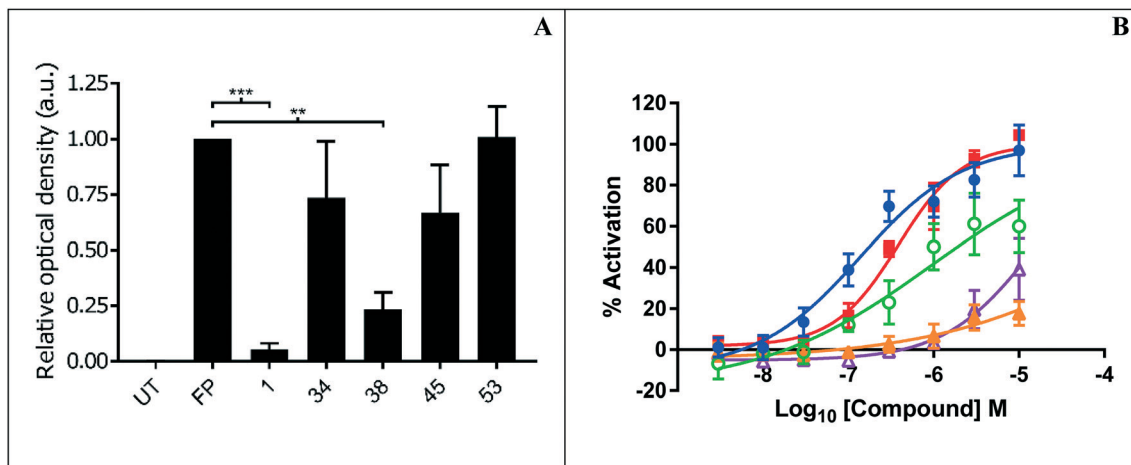


Fig. 2 (A) NOTUM activity-based occupancy assay was performed with FP-biotin (2 μ M) and test compounds (10 μ M) for 10 minutes in conditioned media from HEK293S cells stably transfected with a NOTUM lentiviral construct. Relative occupancy was calculated by optical density of fluorescent band detecting the level of biotinylation of NOTUM using image studio lite 5.2, compared to the control-treated sample which was set to 1. $N = 3$ with S.D. statistical significance is calculated using an unpaired t -test with Welch's adjustment ($***p \leq 0.0005$, $**p \leq 0.005$). UT, untreated. (B) Percentage activation of the Wnt pathway *via* inhibition of NOTUM by compounds in the stable TCF-Lef SuperTOPFLASH luciferase reporter HEK293T cell line. Cells were treated in 8 point concentration response curves from 3 nM to 10 μ M for 18 hours. % activation of the TCF/Lef reporter gene was calculated by normalizing data to DMSO (minimum) and to compound 1 at 10 μ M (maximum) control wells. EC_{50} s were calculated using a 4PL fit in Graphpad prism and Dotmatics studies. Compound key: 1 (●), 37 (■), 38 (○), 45 (▲), 49 (△).

Wnt signaling (EC_{50} 0.138 ± 0.053 μ M; $n = 4$) in this model system through inhibition of NOTUM (ESI, ‡ Table S2). Compound 37 also showed activation of Wnt signaling *via* inhibition of NOTUM (EC_{50} 0.386 ± 0.199 μ M; $n = 4$). Compound 38 demonstrated 60% inhibition of NOTUM at 3 μ M (estimated EC_{50} 0.934 ± 0.657 μ M; $n = 4$), whilst 45 and 49 showed 20% and 38% inhibition at 10 μ M respectively. More stringent EC_{50} determination was precluded by bell shaped dose response curves for the compounds when tested at concentrations > 10 μ M. In contrast, 27 and 35 demonstrated a supra-maximal response consistent with dual activity in this assay, preventing accurate EC_{50} determination. These compounds not only inhibit NOTUM as shown by the Wnt3a-mediated activation of the reporter system but also acts as stabilizers of the luciferase enzyme giving the supramaximal response.²⁹ This luciferase activity is consistent with similar chemical structures to 3 that have been reported to be inhibitors of luciferase in the PubChem database.³⁰

Throughout the course of analogue preparation, preferred examples were assessed for microsomal stability (Table 3). However, the majority of the compounds tested were rapidly metabolized in an NADPH-independent manner with $t_{1/2} < 12.5$ min. One approach to mitigate this issue was to introduce a NMe linker as a direct replacement for the O linker with indazole 53 (*cf.* 34) but this led to a 25-fold decrease in activity and had no effect on alleviating the NADPH-independent metabolism. When an isolipophilic non-aromatic amide was profiled in MLM, tetrahydroisoquinoline 54 was also found to have rapid degradation in a NADPH-independent manner. Even revisiting some of the more polar analogues such as 3 and 22 in MLM suffered a similar outcome. Rapid NADPH-independent metabolism of structurally

related 2-phenoxypropanamides has recently been reported suggesting a common metabolic liability associated with this type of scaffold.³¹ Hence, in light of this work, we recommend assessing the stability of *N*-aryl 2-phenoxyacetamide scaffolds to NADPH-independent metabolism in liver microsomes early in the drug discovery process.

In summary, a crystallographic fragment screen with carboxylesterase NOTUM identified 2-phenoxyacetamide 3 as binding in the palmitoleate pocket with modest inhibition activity. Optimization of hit 3 by SAR studies guided by SBDD identified indazole 38 and isoquinoline 45 as potent inhibitors of NOTUM with properties entirely consistent with CNS drug space. Through direct inhibition of NOTUM, 38 and 45 may prove to be valuable chemical tools for use in *in vitro* disease models where over activity of NOTUM suppressing Wnt signaling is an underlying cause. However, ultimately, it was not possible to combine NOTUM inhibition activity with metabolic stability in this series as the majority of the compounds tested in liver microsomes were rapidly metabolized in an NADPH-independent manner. These compounds represent a step forward in identifying new chemical matter to study the role of NOTUM in Wnt signaling, and work is ongoing to identify compounds suitable for *in vivo* studies to validate NOTUM as a target in Wnt signaling related CNS disorders.

Funding Sources

E. Y. J.: Structural analysis was performed by Y. Z., L. V., R. R. R. and E. Y. J. supported by Cancer Research UK (Programme Grant C375/A17721) and the Wellcome Trust (PhD Training Programme 102164/B/13/Z). The Wellcome Trust funds the Wellcome Centre for Human Genetics, University of Oxford



(Centre Grant 203141/Z/16/Z). P. V. F.: This work was supported by the Alzheimer's Research UK (ARUK) and the Francis Crick Institute. The ARUK UCL Drug Discovery Institute is core funded by Alzheimer's Research UK (520909). The Francis Crick Institute receives its core funding from Cancer Research UK (FC001002), the UK Medical Research Council (FC001002), and the Wellcome Trust (FC001002).

Abbreviations

A β	Amyloid-beta
ABPP	Activity-based protein profiling
AD	Alzheimer's disease
ADME	Absorption distribution metabolism elimination
CNS	Central nervous system
FP	Fluorophosphate
HLM	Human liver microsomes
LE	Ligand efficiency
LLE	Lipophilic ligand efficiency
MLM	Mouse liver microsomes
MPO	Multiparameter optimization
NADPH	Nicotinamide adenine dinucleotide phosphate
OPTS	Trisodium 8-octanoyloxy pyrene-1,3,6-trisulfonate
P-gp	P-Glycoprotein
PTM	Post translational modifications
SAR	Structure activity relationship
SBDD	Structure based drug design
TPSA	Topological polar surface area
UPLC-MS	Ultra performance liquid chromatography – mass spectrometer

Conflicts of interest

There are no conflicts of interest to declare.

Acknowledgements

We thank our colleagues Jamie Bilsland, Will Mahy, Patricia Salinas, Fredrik Svensson, Ed Tate, J. P. Vincent, Paul Whiting, Nicky Willis and Matthias Zebisch of our NOTUM Consortium for their support and advice. The Cell Services and Structural Biology Science Technology Platforms (STPs) at the Francis Crick Institute are gratefully acknowledged for their provision and purification of recombinant NOTUM. We thank Artur Costa, Stefan Constantinou, and Kathryn Costelloe for assistance with the biochemical screening, and Abil Aliev and Kersti Karu at the UCL Department of Chemistry for spectroscopic and analytical services. The authors thank Frank von Delft and the XChem team for enabling the crystallographic fragment screen (beamtime proposal IB16814) and the staff of Diamond Light Source beamlines I04-1 and I24 for assistance with data collection (BAG application MX14744). ADME studies reported in this work were independently performed by GVK Biosciences (Hyderabad, India) and/or Cyprotex (Macclesfield, UK).

References

- 1 R. Nusse and H. Clevers, Wnt/ β -Catenin Signaling, Disease, and Emerging Therapeutic Modalities, *Cell*, 2017, **169**, 985–999.
- 2 C. Niehrs, Function and biological roles of the Dickkopf family of Wnt modulators, *Oncogene*, 2006, **25**, 7469–7481.
- 3 C. Niehrs, The complex world of WNT receptor signaling, *Nat. Rev. Mol. Cell Biol.*, 2012, **13**, 767–779.
- 4 T. Malinauskas and E. Y. Jones, Extracellular modulators of Wnt signaling, *Curr. Opin. Struct. Biol.*, 2014, **29**, 77–84.
- 5 P. Polakis, Wnt signaling in cancer, *Cold Spring Harbor Perspect. Biol.*, 2012, **4**, a008052.
- 6 C.-C. Liu, *et al.* Deficiency in LRP6-Mediated Wnt Signaling Contributes to Synaptic Abnormalities and Amyloid Pathology in Alzheimer's Disease, *Neuron*, 2014, **84**, 63–77.
- 7 A. Marzo, *et al.* Reversal of synapse degeneration by restoring Wnt signaling in the adult hippocampus, *Curr. Biol.*, 2016, **26**, 2551–2561.
- 8 (a) Y. Zhou, *et al.* Canonical WNT signaling components in vascular development and barrier formation, *J. Clin. Invest.*, 2014, **124**, 3825–3846; (b) L. Liu, W. Wan, S. Xia, B. Kalionis and Y. Li, Dysfunctional Wnt/ β -catenin signaling contributes to blood-brain barrier breakdown in Alzheimer's disease, *Neurochem. Int.*, 2014, **75**, 19–25.
- 9 C. Parr, N. Mirzaei, M. Christian and M. Sastre, Activation of the Wnt/ β -catenin pathway represses the transcription of the β -amyloid precursor protein cleaving enzyme (BACE1) via binding of T-cell factor-4 to BACE1 promoter, *FASEB J.*, 2015, **29**, 623–635.
- 10 C. Y. Janda and K. C. Garcia, Wnt acylation and its functional implication in Wnt signaling regulation, *Biochem. Soc. Trans.*, 2015, **43**, 211–216.
- 11 O. Gerlitz and K. Basler, Wingful, an extracellular feedback inhibitor of Wingless, *Genes Dev.*, 2002, **16**, 1055–1059.
- 12 S. Kakugawa, *et al.* NOTUM deacylates Wnt proteins to suppress signaling activity, *Nature*, 2015, **519**, 187–192.
- 13 X. Zhang, *et al.* NOTUM is required for neural and head induction via Wnt deacylation, oxidation, and inactivation, *Dev. Cell*, 2015, **32**, 719–730.
- 14 (a) J. E. Tarver, *et al.* Stimulation of cortical bone formation with thienopyrimidine based inhibitors of NOTUM Pectinacylesterase, *Bioorg. Med. Chem. Lett.*, 2016, **26**, 1525–1528; (b) R. Brommage, *et al.* NOTUM inhibition increases endocortical bone formation and bone strength, *Bone Res.*, 2019, **7**, 2.
- 15 D. T. Manallack, The pKa Distribution of Drugs: Application to Drug Discovery, *Perspect. Med. Chem.*, 2007, **1**, 25–38.
- 16 T. T. Wager, R. Y. Chandrasekaran, X. Hou, M. D. Troutman, P. R. Verhoest, A. Villalobos and Y. Will, Defining desirable central nervous system drug space through the alignment of molecular properties, in vitro ADME, and safety attributes, *ACS Chem. Neurosci.*, 2010, **1**, 420–434.
- 17 D. T. Manallack, R. J. Pranker, E. Yuriev, T. I. Oprea and D. K. Chalmers, The significance of acid/base properties in drug discovery, *Chem. Soc. Rev.*, 2013, **42**, 485–496.



- 18 P. S. Charifson and W. P. Walters, Acidic and basic drugs in medicinal chemistry: a perspective, *J. Med. Chem.*, 2014, **57**, 9701–9717.
- 19 L. Di, H. Rong and B. Feng, Demystifying brain penetration in central nervous system drug discovery. Miniperspective, *J. Med. Chem.*, 2013, **56**, 2–12.
- 20 R. M. Suciu, A. B. Cognetta, Z. E. Potter and B. F. Cravatt, Selective Irreversible Inhibitors of the Wnt-Deacylating Enzyme NOTUM Developed by Activity-Based Protein Profiling, *ACS Med. Chem. Lett.*, 2018, **9**, 563–568.
- 21 <https://www.diamond.ac.uk/Instruments/Mx/Fragment-Screening/Fragment-Libraries.html>. Accessed 18th October 2018.
- 22 J. Barbosa, K. G. Carson, M. W. Gardyan, W. He, V. Lombardo, P. Pabba and J. Tarver Jr Inhibitors of notum pectinacylesterase and methods of their use, *US20120065200*, 2012.
- 23 Z. Rankovic, CNS Drug Design: Balancing Physicochemical Properties for Optimal Brain Exposure, *J. Med. Chem.*, 2015, **58**(6), 2584–2608.
- 24 T. T. Wager, *et al.* Moving beyond Rules: The Development of a Central Nervous System Multiparameter Optimization (CNS MPO) Approach To Enable Alignment of Druglike Properties, *ACS Chem. Neurosci.*, 2010, **1**(6), 435–449.
- 25 Z. Rankovic, CNS Physicochemical Property Space Shaped by a Diverse Set of Molecules with Experimentally Determined Exposure in the Mouse Brain, *J. Med. Chem.*, 2017, **60**(14), 5943–5954.
- 26 Y. Liu, M. P. Patricelli and B. F. Cravatt, Activity-based protein profiling: The serine hydrolases, *Proc. Natl. Acad. Sci. U. S. A.*, 1999, **96**, 14694–14699.
- 27 P. D. Leeson and B. Springthorpe, The influence of drug-like concepts on decision-making in medicinal chemistry, *Nat. Rev. Drug Discovery*, 2007, **6**, 881–890.
- 28 T. W. Johnson, R. A. Gallego and M. P. Edwards, Lipophilic Efficiency as an Important Metric in Drug Design, *J. Med. Chem.*, 2018, **61**, 6401–6420.
- 29 D. S. Auld, N. Thorne, D.-T. Nguyen and J. A. Inglese, Specific Mechanism for Non-Specific Activation in Reporter-Gene Assays, *ACS Chem. Biol.*, 2008, **3**, 463–470.
- 30 N. Thorne, M. Shen, W. A. Lea, A. Simeonov, S. Lovell, D. S. Auld and J. Inglese, Firefly luciferase in chemical biology: A compendium of inhibitors, mechanistic evaluation of chemotypes, and suggested use as a reporter, *Chem. Biol.*, 2012, **19**, 1060–1072. See also: <https://pubchem.ncbi.nlm.nih.gov/substance/7972821#section=Top> Accessed 10th December 2018.
- 31 S. Chacko, *et al.* Expanding Benzoxazole-Based Inosine 5'-Monophosphate Dehydrogenase (IMPDH) Inhibitor Structure-Activity As Potential Antituberculosis Agents, *J. Med. Chem.*, 2018, **61**, 4739–4756.

